

# 1,12-Substituted tetracyclines as antioxidant agents<sup>☆</sup>

Jittiwud Lertvorachon,<sup>a</sup> Jong-Pyung Kim,<sup>b</sup> Dmitriy V. Soldatov,<sup>c</sup> Jason Boyd,<sup>a</sup>  
Gheorghe Roman,<sup>a</sup> Sung Ju Cho,<sup>a,†</sup> Tomasz Popek,<sup>a</sup> Young-Sik Jung,<sup>d</sup>  
Peter C. K. Lau<sup>a</sup> and Yasuo Konishi<sup>a,\*</sup>

<sup>a</sup>National Research Council Canada, Biotechnology Research Institute, 6100 Royalmount Ave., Montréal, QC, Canada H4P 2R2

<sup>b</sup>Korea Research Institute of Bioscience and Biotechnology, Laboratory of Antioxidants, PO Box 115, Yuseong, Taejeon 305-600, Korea

<sup>c</sup>National Research Council Canada, Steacie Institute for Molecular Sciences, 100 Sussex Dr., Ottawa, ON, Canada K1A 0R6

<sup>d</sup>Korea Research Institute of Chemical Technology, PO Box 107, Yuseong, Taejeon 305-600, Korea

Received 23 March 2005; revised 15 April 2005; accepted 15 April 2005

Available online 13 June 2005

**Abstract**—Novel hydroxypyrazoline derivatives of tetracycline and minocycline have been synthesized through the reaction of these tetracyclines with hydrazine. The formation of a new chiral center at C12 is stereospecific to give 12S-12-hydroxy-1,12-pyrazolinotetracycline. A reaction mechanism for the formation of these novel tetracycline derivatives has been proposed. Hydroxypyrazolinotetracyclines exhibit no binding to  $Mg^{2+}$  and  $Zn^{2+}$ , features that are required for antibiotic activity and matrix metalloproteinase (MMP) inhibitions, respectively. The modification toward their hydroxypyrazolino derivatives significantly improved the antioxidant activities of tetracycline and minocycline, as shown by three commonly used assays (DPPH, ABTS<sup>•+</sup>, and superoxide scavenging). 12S-Hydroxy-1,12-pyrazolinominocycline is a promising tetracycline-based antioxidant devoid of antibiotic properties and MMP inhibitory activity, which could be beneficial in the treatment of complications related to oxidative stress.  
Crown Copyright © 2005 Published by Elsevier Ltd. All rights reserved.

## 1. Introduction

Free radicals are very reactive species that are routinely generated in living organisms in a variety of normal metabolic processes and in much larger amounts during chronic or acute insults. An organism's immune system can make good use of free radicals, and these species also act as signal molecules, which trigger and regulate cellular processes through subtle changes in redox balance. However, excess amounts of free radicals can cause cell disruption and death by reacting with important cellular components, such as nucleic acids, membrane lipids, or proteins, and mediate a wide range of diseases and conditions such as atherosclerosis,<sup>1</sup> inflammation,<sup>2</sup> carcinogenesis,<sup>3</sup> rheumatoid arthritis,<sup>4</sup> cataract,<sup>5</sup> asthma,<sup>6</sup> Parkinson's disease,<sup>7</sup> Alzheimer's

disease,<sup>8,9</sup> diabetes,<sup>10</sup> and glycation complications.<sup>11</sup> In response to the excess of free radicals, living organisms have developed complex and efficient natural free radical defense systems, including enzymes such as superoxide dismutase (SOD), glutathione peroxidase (GPx), glutathione reductase (GR), catalase, and several metalloenzymes (e.g., ferritin or ceruloplasmin), or nonenzymatic antioxidants such as glutathione, vitamin E, vitamin C, carotenoids, etc., to either quench or transform free radicals into less reactive forms, or, indirectly, to regulate the biosynthesis of antioxidant proteins. A living organism's natural antioxidant systems must be continuously maintained and replenished because antioxidants are largely a preferred target for free radicals. Moreover, these systems have been naturally designed to work as a whole in which each component functions in close harmony with the others, as antioxidants should be active either in aqueous or in lipid environments and they should be able to protect in the same time the membrane and the cytoplasm. Such an example of synergistically enhanced natural antioxidant system is the regeneration of  $\alpha$ -tocopherol by vitamin C, which in turn is recycled by the dihydrolipoate–lipoate couple, that is finally restored by the NAD–NADH system.<sup>12,13</sup>

**Keywords:** Tetracyclines; Pyrazole derivatives; Antioxidant.

<sup>☆</sup>NRC Publication No. 47469.

\* Corresponding author. Tel.: +1 514 496 6339; fax: +1 514 496 5143; e-mail: [yasuo.konishi@nrc-nrc.gc.ca](mailto:yasuo.konishi@nrc-nrc.gc.ca)

<sup>†</sup>Current address: Department of Pharmacology and Therapeutics, McGill University, 3655 Promenade Sir-William-Osler, Montréal, QC, Canada H3G 1Y6.

A special feature of the natural antioxidant systems is their defensive strategy based on the ability to regenerate the first line of antioxidants (vitamin E, vitamin C, superoxide dismutase, etc.) by using endogenous or exogenous redox compounds. The general consensus is that constant replacement of antioxidants in the first line of defense through the intake of fresh fruits and vegetables, or supplements that include nutraceuticals such as vitamin E, vitamin C or carotenoids, and nonnutrient antioxidants (e.g., flavonoids), is highly beneficial. However, the efficiency of the natural antioxidant systems is often challenged by personal factors such as genetically inherited resistance, physical and emotional stress, age, and, chiefly, by diseases. In situations when more radicals are produced than the natural antioxidant systems can counteract, therapeutic use of antioxidants is required. At this point, it is worth stating that placing one's bet on a sole therapeutic antioxidant as being a sort of *panacea universalis* against free radicals is unrealistic. Each and every antioxidant may exhibit distinct mechanisms of action such as radical scavenging, chain-breaking, or ion metal chelation, different affinities for various types of free radicals, a characteristic behavior in terms of membrane permeability. Hence, therapeutic antioxidants should be designed for specific purposes and taken as complements to their natural counterparts.

Some tetracyclines are well-known antibiotics against a wide range of aerobic and anaerobic Gram-positive and Gram-negative bacteria. The antibiotic activity of tetracyclines is associated with their ability to bind to the 30S ribosomal subunit of bacterial RNA and inhibit the binding of aminoacyl-tRNA to ribosomes that leads to the blockage of bacteria protein synthesis.<sup>14</sup> The manifestation of the antibiotic properties of tetracyclines requires the coordination of  $Mg^{2+}$  to the 1,3-ketoenol moiety residing between C11 and C12.<sup>‡</sup> Apart from their antibiotic action, tetracyclines inhibit matrix metalloproteinases (MMPs), a characteristic that requires coordination to  $Zn^{2+}$  through the same 1,3-ketoenol moiety.<sup>15</sup>

Over 7000 tetracyclines have been reported and most of these compounds have been isolated or synthesized as a part of an ongoing effort to look for better antibiotics. However, little has been done toward the chemical modification of the lower peripheral region comprising C1, C11, and C12 (Fig. 1). The lack of interest in modifying the lower peripheral region of tetracyclines can be accounted for by the observation that this part of the molecule is essential for both antibiotic activity and MMPs inhibition, which have been until now the major clinical applications of these compounds. On the contrary, when tetracyclines become of interest for applications other than antibiotic or MMPs inhibition, the antibiotic activity may lead to the development of antibiotic-resistant microorganisms during prolonged use, or the MMPs inhibition may cause undesired feed-

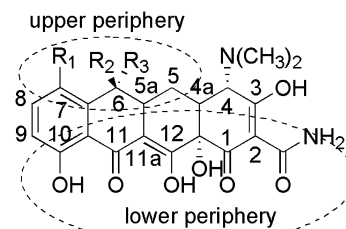


**Figure 1.** Designation of upper and lower peripheral regions in tetracyclines.

back.<sup>16</sup> In relation to this, the transformation of the substructure extending over C1, C11, and C12 in the lower peripheral region of rings A, B, and C may be attractive in order to eliminate the antibiotic and MMPs inhibition activities.

This paper reports the chemical modification of C1 and C12 in minocycline and tetracycline through reaction with hydrazine, with the aim of improving these two compounds' antioxidant activity while eliminating their antibiotic and MMPs inhibitory activities.

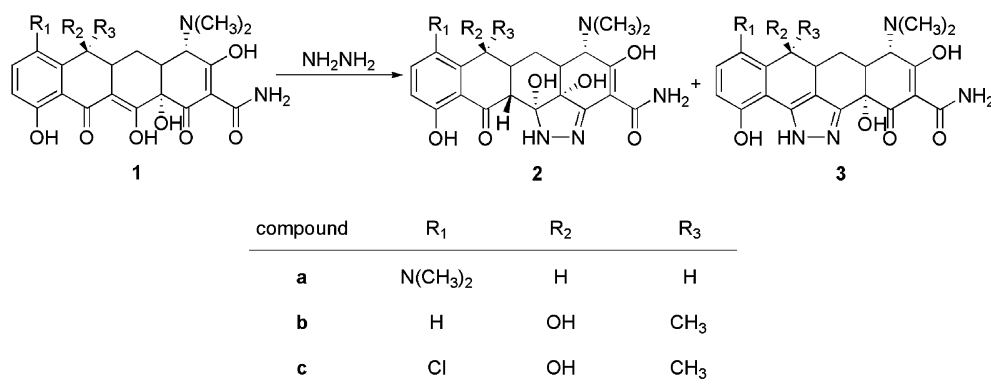
## 2. Results and discussion

### 2.1. Chemistry

The modification of C1, C11, and C12 in tetracyclines can be achieved through reaction with reagents specific to carbonyl groups, such as hydrazine. The three ketone groups at C1, C11, and C12 form two 1,3-keto-enol substructures, and the reaction of such substructures with hydrazine is known to lead to pyrazole derivatives through ring closure.<sup>17</sup> When minocycline hydrochloride **1a** was stirred with 2.5 equiv of hydrazine hydrate in water at room temperature overnight, the HPLC analysis of the crude reaction mixture revealed the presence of two major reaction products in a 1:1 ratio. Their HPLC separation afforded two novel minocycline derivatives **2a** and **3a** in approximately 40% yield each. However, the attempt to apply the same reaction conditions to tetracycline hydrochloride gave only one reaction product **3b**, which was identified as 11,12-pyrazolotetracycline<sup>18</sup> known as CMT-5 and deemed structurally related to **3a** based on its UV absorption. Refluxing tetracycline hydrochloride with 2.5 equiv of hydrazine hydrate in ethanol for 3 h led to the formation of two reaction products in a 3:1 ratio, the most abundant being **3b** (54%). The other reaction product was **2b**, which was designated as the tetracycline version of **2a** based on the similarities of these two compounds' UV absorptions. The reaction of chlortetracycline with hydrazine hydrate under various conditions led only to the isolation of the corresponding 11,12-pyrazolochlortetracycline.<sup>18</sup>

The structural assignment as 12S-12-hydroxy-1,12-pyrazolotetracycline for **2b** relied on the corroborated information provided by mass spectrometry, <sup>1</sup>H, and <sup>13</sup>C NMR investigations and single-crystal XRD

<sup>‡</sup> The numbering throughout the text corresponds to the numbering of the tetracycline ring system in Figure 1.



**Scheme 1.** Reaction of tetracyclines with hydrazine.

analysis. **Scheme 1** illustrates the formation of the two pyrazole derivatives of tetracyclines **1** through ring closure involving C1–C12 and C11–C12 keto-enol substructures, respectively.

According to the generally accepted mechanism for pyrazole ring closure reaction starting from  $\beta$ -diketones,<sup>19,20</sup> the formation of these two pyrazole derivatives of tetracyclines could be drawn as having the addition of hydrazine to the carbonyl group at C11 as the first step, to give **4** and **5** as a result of the nucleophile's attack from above and from below the plane of the naphthacene ring system, respectively (**Scheme 2**). A brief analysis of tetracycline's conformation reveals that the access of hydrazine from below the naphthacene plane is less hindered; it is fair to conclude that the adduct **5** arising from this favored pathway will be produced in higher amount than its isomer **4**. Keto-enol tautomerization at C12 would provide a carbonyl function suitably located for the pyrazole ring closure to occur, thus affording dihydroxypyrazolidines **6** and **7**. Dehydration of dihydroxypyrazolidines **6** and **7** affords through a slow kinetic controlling step 11,12-pyrazolotetracycline **3b**, which is easily converted to **8** due to the prototropic tautomerism of pyrazoles.

Hydroxypyrazolotetracycline **2b** is produced as a result of a parallel mechanistic pathway (**Scheme 3**). Dihydroxypyrazolidine **6** may undergo a ring opening to adduct **9**, which may be conceived as arising from the formal addition of hydrazine to a ketone function at C12. This adduct can cyclize back to dihydroxypyrazolidine **6** or can nucleophilically attack the ketone group at C1 from above the plane of the naphthacene ring system to produce dihydroxypyrazolidine **10**, which loses only one molecule of water in a slow process that leads to hydroxypyrazolotetracycline **2b**. In this case, the ring closure of the pyrazole ring seems to have arrested in an intermediate stage and the aromatization of the pyrazole ring did not occur as for **3b**. The second dehydration step leading to the fully aromatized pyrazole derivative is prevented because the steric requirements for this process are not fulfilled. The dehydration of **2a** by treatment with a strong dehydrating agent such as *p*-toluenesulfonic acid was unsuccessful.

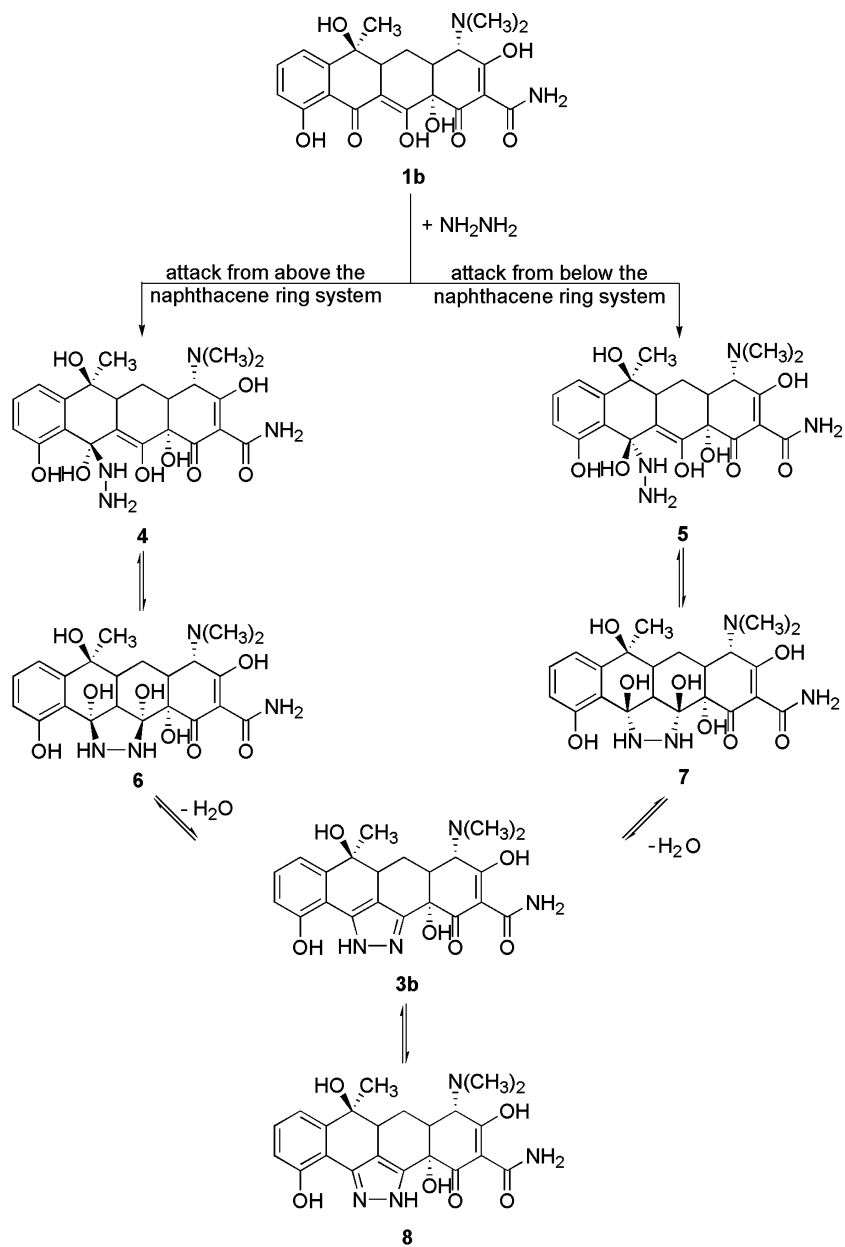
The same type of ring opening observed for dihydroxypyrazolidine **6** is also plausible for its isomer **7**. However, the hypothetical adduct isomeric to **9** arising from this process is supposed to attack the ketone function at C1 from below the plane of the naphthacene ring, a process which is very unlikely to occur due to the steric hindrance exerted by the neighboring hydroxyl group at C12a. According to the X-ray analysis, the only stereoisomer of hydroxypyrazolotetracycline **2b** that was isolated was found to display the hydroxyl group at C12a *anti* to the hydrogen at C11a, making the formation of hydroxypyrazolotetracycline **2b** stereospecific.

According to the proposed mechanism, 11,12-pyrazolotetracycline **3b** is produced at the end of both pathways that are initially defined by the direction of hydrazine's attack onto tetracycline, whereas hydroxypyrazolotetracycline **2b** is the final product resulted from a derivation of only one of the two possible pathways. This could explain the prevalence of pyrazolotetracycline **3b** over hydroxypyrazolotetracycline **2b** that has been noted in all the experiments.

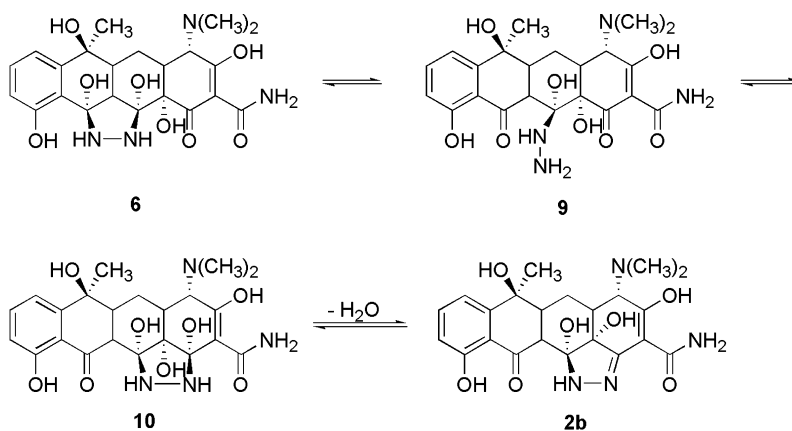
The reaction mechanism depicted in **Schemes 2 and 3** applies to minocycline as well. However, minocycline lacks the methyl and hydroxyl groups at position 6, a structural detail that diminishes the steric hindrance in that region of the molecule and allows the initial attack of hydrazine at C11 to proceed with comparable odds both from above and from below the naphthacene ring system. Consequently, the preference for one pathway is less obvious, and the amounts of hydroxypyrazolominocycline **2a** and pyrazolominocycline **3a** become fairly equal.

## 2.2. Structure of compound **2b** in the crystal

Molecular structure of compound **2b** as inferred from the single-crystal XRD analysis is given in **Supplementary data**. The main change from tetracycline free base<sup>21</sup> is the presence of an additional five-membered ring (ring E). Furthermore, the double bond C11a–C12 in the original tetracycline becomes single in the compound of this study, resulting in two additional chiral centers at C11a and C12. The geometry of the E ring is consistent with the formation of a double bond C1–N1 (1.291(3) Å), a single N1–N12 bond (1.412(3) Å), and



**Scheme 2.** Mechanistic pathway for the formation of 11,12-pyrazolotetracyclines.



**Scheme 3.** Mechanistic pathway for converting intermediate dihydropyrazolidine **6** into hydroxypyrazoline **2b**.

a single C12–N12 bond (1.485(3) Å), with the C1–N1–N12 and N1–N12–C12 angles (108.0(2)° and 107.6(2)°, respectively) being very close to tetrahedral. The C12 hydroxyl group in **2b** occupies space below the plane of the naphthacene ring system, whereas the hydrogen atom at C11a lies above the plane of the ring system. The molecule exists in a nonionized (rather than zwitterionic) form and displays extensive intramolecular hydrogen bonding. As it was discussed before,<sup>22,23</sup> such a form presents a molecular species of reduced polarity and better lipid phase solubility, the factors contributing to a higher biological activity of the compound in such environment. The additional E ring in the structure of compound **2b** creates some restrictions on the conformational flexibility, but does not affect the inter-conversion between conformations, which occurs upon rotation about the C4a–C12a single bond.

### 2.3. Antibiotic activity

The currently-in-use tetracyclines are drugs used to fight infections caused by bacteria. However, long-term widespread and heavy use of tetracyclines has spurred evolutionary changes in bacteria that allow them to survive these powerful drugs and promote the extent of antibiotic resistance. In order for pyrazolotetracyclines to be used as antioxidant agents, these compounds should lack the antibiotic property of the parent tetracyclines.

The antibiotic activity of tetracyclines is associated with reversible inhibition of protein synthesis, which is accomplished by interfering with the binding of aminoacylated tRNA to the A-site of the 30S subunit of the ribosome.<sup>24</sup> Three-dimensional structures available for the 30S and characterizing specific tetracycline–protein interactions<sup>25</sup> show that the chelation of Mg<sup>2+</sup> to tetracyclines is crucial in this respect.<sup>26</sup> Indeed, 11,12-pyrazolotetracyclines **3b** and **3c**, which can no longer bind Mg<sup>2+</sup> due to their chemical modification, were more than 200-fold less active than tetracycline.<sup>18</sup> The antibiotic activity of the compounds **1a,b**, **2a**, and **2b** was measured by the growth inhibition of tetracycline sensitive and resistant bacteria, BL21(DE3), and XL2-Blue, respectively. Tetracycline was shown to have antibiotic activity against BL21(DE3) at concentrations ranging from 10 to 60 µg/mL, but its antibiotic activity was concentration dependent in the case of XL2-Blue strain, whose growth was only partly inhibited even at the highest concentration (Table 1). Minocycline presented antibiotic activity against both tetracycline sensitive and resistant bacteria strains, even at the lowest concentration used in this assay. Hydroxypyrazolinotetracyclines **2a** and **2b** proved to lack any antibiotic activity against both tetracycline sensitive and resistant bacteria strains at concentrations ranging from 10 to 60 µg/mL. Similarly, growth curves (data not shown) confirmed that **2a** and **2b** did not affect the growth rate of the *Escherichia coli* strains tested as compared with their growth in media alone.

### 2.4. Zn<sup>2+</sup> binding assay

Tetracyclines inhibit MMPs activity,<sup>27,28</sup> but also interfere with the transcription and activation steps of

**Table 1.** Antibiotic activity of compounds **1a,b**, **2a**, and **2b** against tetracycline sensitive and resistant bacteria (BL21(DE3) and XL2-Blue, respectively)

Compound	µg/mL	BL21(DE3)	XL2-Blue
<b>1a</b>	10	— <sup>a</sup>	— <sup>a</sup>
	20	—	—
	40	—	—
	60	—	—
<b>1b</b>	10	—	+++
	20	—	+++
	40	—	+++
	60	—	+
<b>2a</b>	10	++++	++++
	20	++++	++++
	40	++++	++++
	60	++++	++++
<b>2b</b>	10	++++	++++
	20	++++	++++
	40	++++	++++
	60	++++	++++

<sup>a</sup> Relative growth of bacterial strains when incubated in the presence of **1a,b**, **2a** and **2b**. (++++ indicates 100% growth and (—) indicates no growth as compared to antibiotic-free media. Strain genotypes are: BL21(DE3), *E. coli* B F<sup>−</sup> dcm ompT hsdS(r<sub>B</sub>, m<sub>B</sub>) gal λ(DE3). XL2-Blue, recA1 endA1 gyrA96 thi-1 hsdR17 supE44 relA1 lac [F' proAB lacIqZAM15 Tn10(Tetr) Amy Camr].

MMPs.<sup>29–31</sup> The effect of tetracyclines on MMPs activity is thought to be due directly to the chelation of Zn<sup>2+</sup>,<sup>32,33</sup> as MMPs are dependent on Zn<sup>2+</sup> to activate and maintain their active tertiary structure<sup>34</sup> and hydrolytic activity.<sup>35</sup> Up to now, Zn<sup>2+</sup> chelation site(s) to tetracyclines is still an unresolved problem, and only indirect information has been used to assign one of the sites that are subject to protonation–deprotonation equilibria or evaluate the contribution of the possible donor atoms as relevant in the formation of Zn<sup>2+</sup>–tetracyclines complexes. Studies have presented tetracyclines as chelators of Zn<sup>2+</sup>,<sup>36,37</sup> and different reactivities of these drugs toward Zn<sup>2+</sup> have been assessed under physiological conditions<sup>38</sup> and postulated to be associated with the presence of phenol–diketone moiety in the lower peripheral part of the molecule.<sup>39</sup> The tentative assignment of the Zn<sup>2+</sup> binding site to tetracyclines as the C11–C12 diketone function is grounded on the finding that the addition of Zn<sup>2+</sup> to CMT-5 **3b**, which lacks the C11–C12 diketone moiety, neither altered the peak height nor shifted its absorption maxima.<sup>15</sup> Furthermore, CMT-5 is the only tetracycline unable to inhibit the activity of MMPs, a characteristics that can be correlated to the absence of the Zn<sup>2+</sup> binding site in the structure of this particular type of chemically modified tetracycline.<sup>27,33</sup>

The inadequacy of pyrazolominocycline **3a** having an identical structural modification as CMT-5 to bind to Zn<sup>2+</sup> has been confirmed by the UV–vis absorbance measurements (data not shown). Hydroxypyrazolinotetracyclines **2a** and **2b** were also investigated in this respect by UV–vis spectroscopy. The absorption spectra of tetracyclines exhibit characteristic features within the wavelength range of 300–450 nm that are altered when these compounds form complexes with divalent cations at chromophore BCD.<sup>40</sup> The absorption spectra of



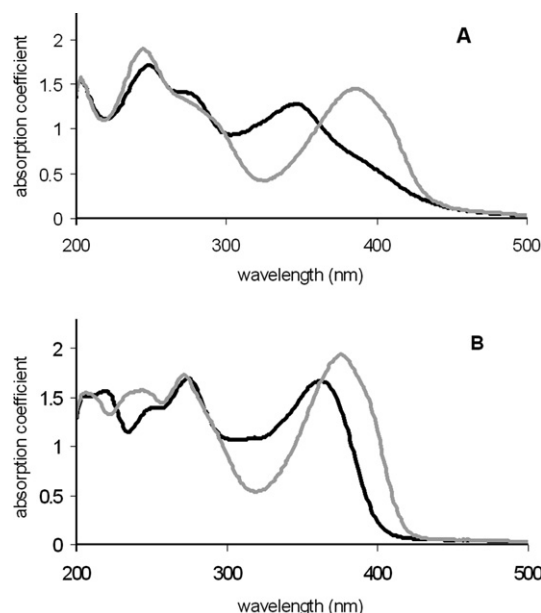


**Figure 2.** UV spectra of minocycline hydrochloride **1a** (A) and tetracycline hydrochloride **1b** (B) in the absence (—) and in the presence (—) of  $\text{Zn}^{2+}$  (0.1 M).

tetracycline and minocycline are presented in Figure 2. Tetracycline showed absorption maximum at 362 nm in the absence of divalent cations. Addition of the equimolar or higher amount of  $\text{Zn}^{2+}$  shifted the absorption maximum to 375 nm, and the absorption coefficient increased by 17%. In a similar way, minocycline presented absorption maximum at 344 nm in the absence of divalent cations. Addition of  $\text{Zn}^{2+}$  induced a bathochromic shift to 383 nm, and the absorption coefficient increased by 13%. Modification of chromophore BCD in hydroxypyrazolinotetracyclines **2** by creating the additional heterocyclic ring led to a hypsochromic shift of the absorption peak from 344 nm to 312 nm for compound **2a** and from 362 nm to 317 nm for compound **2b**. The changes in terms of absorption wavelength and coefficient on addition of  $\text{Zn}^{2+}$  were minimum (Fig. 3), proving that no binding of hydroxypyrazolinotetracyclines **2** to  $\text{Zn}^{2+}$  occurred. Like CMT-5, hydroxypyrazolinotetracyclines **2** do not bind to  $\text{Zn}^{2+}$ , therefore are devoid of inhibitory action on MMPs.

## 2.5. Antioxidant activity

Several protocols for antioxidant assays have been elaborated to measure the extent of scavenging pre-formed radicals by hydrogen- or electron-donation using a broad range of conditions, oxidants, manners to measure oxidation, and end-points of oxidation.<sup>41</sup>

2,2-Diphenyl-1-picrylhydrazyl (DPPH) assay measures the hydrogen-donating ability of antioxidants to convert stable DPPH free radical to 1,1-diphenyl-2-picrylhydrazine.<sup>42</sup> The reaction is accompanied by a change in color from deep-violet to light-yellow and is monitored spectrophotometrically. Trolox and butylated hydroxyanisole (BHA) usually serve as reference antioxidants in this assay.

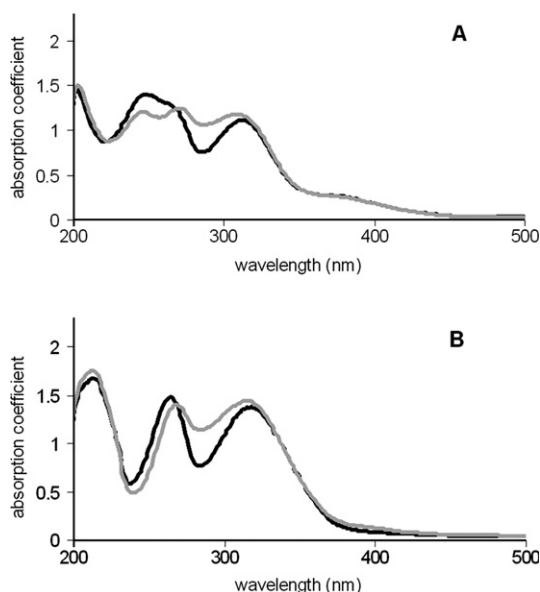


**Figure 3.** UV spectra of hydroxypyrazolinomincycline **2a** (A) and hydroxypyrazolinotetracycline **2b** (B) in the absence (—) and in the presence (—) of  $\text{Zn}^{2+}$  (0.1 M).

2,2'-Azinobis (3-ethylbenzothiazoline-6-sulfonate) (ABTS) assay involves long-lived ABTS radical cation, which is chemically produced by the oxidation of the corresponding colorless sulfonic acid with potassium persulfate. The green-blue  $\text{ABTS}^{\cdot+}$  radical has excellent spectral characteristics, is stable over a wide range of pH, and is applicable to the study of both water-soluble and lipid-soluble antioxidants that convert  $\text{ABTS}^{\cdot+}$  back to the initial sulfonic acid.<sup>43</sup>

Superoxide assay consists on the irradiation of riboflavin in the presence of EDTA and methionine as electron donor to produce photochemically reduced flavin, which subsequently reduces atmospheric oxygen to superoxide radical anions.<sup>44</sup> Superoxide radical anions further reduce nitroblue tetrazolium (NBT) into formazan, whose formation is monitored spectrophotometrically. In vivo, xanthine oxidase is one of the enzymatic sources of superoxide radical anion through the reduction of oxygen dissolved in body fluids.

Table 2 resumes the results for the antioxidant activity of parent tetracyclines **1a** and **1b** and hydroxypyrazolinotetracyclines **2a** and **2b** in DPPH,  $\text{ABTS}^{\cdot+}$  and superoxide assays. Pyrazolotetracycline **3b** and reference compounds, butylated hydroxyanisole (BHA), and trolox are also included in Table 2.

The phenolic hydroxyl in ring D of tetracyclines is the most reactive site in scavenging free radicals. The phenoxyl radical generated by the radicals employed in the assays is stable, and its stability is further enhanced by the presence of the electron-donating 7-dimethylamino group. Indeed, minocycline **1a** and its hydroxypyrazolino derivative **2a** showed high antioxidant activity in all three assays, while tetracycline is a much weaker antioxidant. The hydroxypyrazolino moiety in **2** improves the antioxidant activity of the parent tetracyclines **1** in

**Table 2.** In vitro antioxidant activity of tetracyclines (EC<sub>50</sub> in  $\mu\text{M}$ ) in DPPH, ABTS<sup>•+</sup> and superoxide radical anion scavenging assays

Compound	DPPH ( $\mu\text{M}$ )	ABTS <sup>•+</sup> ( $\mu\text{M}$ )	Superoxide radical ( $\mu\text{M}$ )
<b>1a</b>	20	15	33
<b>1b</b>	1000	>1000	>1000
<b>2a</b>	19	3.6	58
<b>2b</b>	320	69	2300
<b>3b</b>	9200	350	53
BHA	49	11	8.9
Trolox	7.9	13	920

DPPH and ABTS<sup>•+</sup> assays, but not in superoxide assay. On the contrary, the presence of the pyrazole ring in **3b** significantly improves the antioxidant activity of the parent tetracycline **1b** in superoxide assay, but not in DPPH or ABTS<sup>•+</sup> assays. The presence of the extra heterocyclic ring and the supplementary >NH and –OH functions in compounds **2** enhance their antioxidant activity by their ability to act as electron donors. Moreover, hydroxypyrazolinotetracyclines **2** are able to chelate Cu<sup>2+</sup> (data not shown), a known catalyst of free radical formation, thus contributing to the oxidative stress drive.

There is an obvious advantage deriving from the use of hydroxypyrazolinomincycline **2a** as antioxidant over minocycline itself: the lack of antibiotic activity will not trigger the development of minocycline-resistant microorganisms during the chronic use.<sup>45</sup> Taking into account the recent disclosure of failures of MMP inhibitors in clinical trials,<sup>46</sup> the inability of compound **2a** to inhibit MMPs may be beneficial in vivo. However, it should be noted that compound **2a** may still inhibit oxidative activation of pathological MMPs,<sup>47</sup> as compound **3b** does.<sup>28</sup> Furthermore, due to its close structural similarity to minocycline, compound **2a** may have similar adsorption, distribution, metabolism, excretion, and toxicity (ADMET) properties.<sup>48</sup> Thus, compound **2a** may be a lead antioxidant for the treatment of complications related to oxidative stress.

### 3. Conclusion

Novel hydroxypyrazolinotetracyclines have been synthesized through the reaction of tetracycline and minocycline with hydrazine hydrate. The ring closure reaction that used the C12–C1 keto-enol substructure was shown to be stereospecific and led to 12*S*-12-hydroxy-1,12-pyrazolinotetracycline as the only isolated isomer. A possible reaction mechanism was proposed to explain the formation of hydroxypyrazolinotetracyclines along with the known 11,12-pyrazolotetracyclines. The novel hydroxypyrazolinotetracyclines lack any antibiotic activity against both tetracycline sensitive and resistant bacteria strains at concentrations ranging from 10 to 60  $\mu\text{g/mL}$ , and the growth curves confirmed that these compounds do not affect the growth rate of the *E. coli* strains tested as compared with their growth in media alone. The UV–vis spectra of hydroxypyrazolinotetracyclines showed no changes in terms of absorption

wavelength and coefficient upon addition of Zn<sup>2+</sup>, offering proofs of these compounds' inability to chelate this metal ion, a feature which is essential for the inhibition of the transcription and activation of MMPs. Hydroxypyrazolinotetracyclines showed higher antioxidant activity in DPPH, ABTS<sup>•+</sup>, and superoxide assays when compared with the parent tetracyclines due to the presence of the extra heterocyclic ring and the supplementary >NH and –OH functions. Lacking the antibiotic property of tetracyclines and being devoid of MMPs inhibitory activity, hydroxypyrazolinotetracyclines are promising antioxidants useful in the treatment of diseases involving oxidative stress.

## 4. Experimental

### 4.1. Materials and methods

Tetracycline hydrochloride **1b** was purchased from ICN Biomedicals, Inc. (Aurora, OH). Minocycline **1a**, hydrazine hydrate, DPPH free radical, riboflavin, ethylenediaminetetraacetic acid (EDTA), methionine, nitroblue tetrazolium (NBT), dimethylsulfoxide (DMSO), butylated hydroxyanisole (BHA), trolox, 2,2'-azino-bis(3-ethylbenzthiazoline-6-sulfonic acid (ABTS), and potassium persulfate were supplied by Sigma (St. Louis, MO). Chlortetracycline hydrochloride **1c** was provided by Fluka (Buchs, Switzerland). The bacterial strains used in this study were acquired from Stratagene, Canada. Zinc sulfate heptahydrate was an Anachemia (Montréal, Canada) product. HPLC-grade water, acetonitrile, and methanol were purchased from J. T. Baker (Phillipsburg, NJ). Melting points were determined by Electro-thermal Melting Point apparatus (Sigma–Aldrich, Oakville, Canada) and are uncorrected. <sup>1</sup>H NMR spectra were recorded on Bruker Advance 500 spectrometer. Molecular mass determination was carried out on an API III electrospray mass spectrometer (Sciex, Concord, ON, Canada) and on a Micromass Q-TOF Global spectrometer (Waters, Milford, MA). The purity of all synthetic products ( $\geq 98\%$ ) was established by HPLC using an analytical C18-reverse phase SymmetryShield<sup>TM</sup> column (3.5  $\mu\text{m}$ ; 4.6  $\times$  50 mm). The method used a binary gradient of 0.1% trifluoroacetic acid (TFA) in water (phase A) and 0.1% TFA in acetonitrile (phase B) on a gradient from 0% phase B at time 0 to 80% phase B at 10 min at a flow rate of 1.5 mL/min. The single-crystal XRD analysis was performed on a Bruker SMART CCD X-ray diffractometer. A DU<sup>®</sup> 640 spectrophotometer (Beckman Coulter, Inc., Fullerton, CA) was used to monitor the optical densities of bacteria cultures. The absorption spectra were recorded on a Varian (Cary 3E) UV–vis spectrophotometer. A tunable microplate reader Versa<sub>max</sub> (Molecular Devices, CA) was used to measure the antioxidant activity.

### 4.2. Synthesis of hydroxypyrazolinomincycline **2a** and pyrazolomincycline **3a**

Minocycline hydrochloride **1a** (50 mg, 0.10 mmol) was suspended in water (1.25 mL), then hydrazine hydrate (17.5  $\mu\text{L}$ , 0.36 mmol) was added, and the reaction

mixture was stirred at room temperature overnight under nitrogen for 16 h. After the solvent had been removed by freeze drying, the crude product was separated using a C18-reverse phase Vydac column (50 × 250 mm). By applying a binary gradient of 0.1% TFA in water (phase A) and 0.1% TFA in acetonitrile (phase B) on a gradient from 0% phase B to 5% phase B in 100 min at a flow rate of 20 mL/min, compound **2a** (30.6 mg, 52%) separated as a trifluoroacetate. Compound **3a** (22.4 mg, 39%) eluted soon afterwards under isocratic conditions (95% phase A, 5% phase B, 20 mL/min). After freeze drying the collected fractions, the solid material was dissolved in the minimum amount of water and treated with the required amount of triethylamine. The tetracycline derivatives were separated from the water-soluble salts using PrepSep™-C18 disposable extraction columns.

**4.2.1. [5S-(5 $\alpha$ ,5 $\alpha\alpha$ ,6 $\alpha\alpha$ ,12 $\beta\alpha$ ,12 $\alpha$ )]-5,8-Bis(dimethylamino)-1,5,5 $\alpha$ ,6,6 $\alpha$ ,7,12,12 $\alpha$ ,12 $\beta$ ,12 $\gamma$ -decahydro-4,11,12 $\beta$ ,12 $\gamma$ -tetrahydroxy-12-oxo-1,2-diaza-cyclopenta[de]naphthacene-3-carboxylic acid amide **2a**.** Yellowish powder, mp 190 °C (dec).  $t_R$  = 2.8 min.  $^1\text{H}$  NMR (500 MHz,  $\text{D}_2\text{O}$ ):  $\delta$  1.55 (q, 1H,  $J$  = 12.7 Hz), 2.22 (d, 1H,  $J$  = 10.9 Hz), 2.47 (m, 1H), 2.74 (dd, 1H,  $J$  = 13.0 and 15.3 Hz), 2.87 (m, 1H), 3.02 (s, 6H), 3.03 (m, 1H), 3.19 (d, 1H,  $J$  = 13.6 Hz), 3.28 (s, 6H), 3.86 (s, 1H), 7.12 (d, 1H,  $J$  = 9.1 Hz), 7.91 (d, 1H,  $J$  = 9.1 Hz).  $^{13}\text{C}$  NMR (100 MHz,  $\text{CD}_3\text{OD}$ ):  $\delta$  29.0, 33.1, 34.1, 35.6, 42.3, 43.4, 53.4, 68.9, 78.0, 98.5, 114.8, 116.7, 128.5, 137.8, 142.5, 149.8, 158.3, 170.5, 171.0, 185.0, 203.4. HRMS (ESI-TOF) calcd for  $\text{C}_{23}\text{H}_{29}\text{N}_5\text{O}_6$  472.2198 ( $\text{MH}^+$ ). Found 472.2196.

**4.2.2. [6S-(2 $\beta\alpha$ ,6 $\alpha$ ,6 $\alpha\alpha$ ,7 $\alpha\alpha$ )]-6,9-Bis(dimethylamino)-1,2 $\beta$ ,3,6,6 $\alpha$ ,7,7 $\alpha$ ,8-octahydro-2 $\beta$ ,5,12-trihydroxy-3-oxo-1,2-diazacyclopenta[fg]naphthacene-4-carboxylic acid amide **3a**.** Yellowish powder, mp 195–199 °C (dec).  $t_R$  = 4.0 min.  $^1\text{H}$  NMR (500 MHz,  $\text{D}_2\text{O}$ ):  $\delta$  1.53 (q, 1H,  $J$  = 11.5 Hz), 2.12 (t, 1H,  $J$  = 15.1 Hz), 2.24 (d, 1H,  $J$  = 11.4 Hz), 2.96 (s, 6H), 3.06 (m, 2H), 3.20 (br s, 7H), 3.95 (s, 1H), 6.93 (d, 1H,  $J$  = 8.9 Hz), 7.42 (d, 1H,  $J$  = 8.9 Hz).  $^{13}\text{C}$  NMR (100 MHz,  $\text{CD}_3\text{OD}$ ):  $\delta$  29.8, 30.5, 34.5, 36.5, 43.1, 44.7, 73.3, 98.7, 110.2, 113.9, 115.7, 120.2, 129.3, 132.6, 143.4, 145.4, 150.3, 154.0, 159.2, 173.5, 192.6. MS (ESI),  $m/z$ : 454.3 ( $\text{MH}^+$ ). HRMS (ESI-TOF) calcd for  $\text{C}_{23}\text{H}_{27}\text{N}_5\text{O}_5$  454.2090 ( $\text{MH}^+$ ). Found 454.2097.

### 4.3. Synthesis of hydroxypyrazolinetetracycline **2b** and pyrazolotetracycline **3b**

Tetracycline hydrochloride **1b** (200 mg, 0.42 mmol) was suspended in 8 mL absolute ethanol, then hydrazine hydrate (50  $\mu\text{L}$ , 1.04 mmol) was added, and the reaction mixture was refluxed for 3 h. The crude mixture was evaporated to dryness and subjected to high vacuum to remove any traces of solvent. Water (0.8 mL) was added to dissolve the dry residue and, after a few minutes of stirring at room temperature, a beige precipitate formed. The stirring continued for 1 h, the precipitate was then collected and dried (160 mg). The material was dissolved in 3.0 mL of 20% acetic acid and was separated using a C18-reverse phase Vydac column

(50 × 250 mm) employing 0.6% acetic acid in water as mobile phase at a flow rate of 20 mL/min. After freeze drying the collected fractions, the solid materials were dissolved in the minimum amount of water and treated with the required amount of triethylamine. The tetracycline derivatives were separated from the water-soluble salts using PrepSep™-C18 disposable extraction columns. The isolated amount of **2b** was 12.9 mg (6%), whereas the amount of compound **3b** was 125 mg (68%).

**4.3.1. [5S-(5 $\alpha$ ,5 $\alpha\alpha$ ,6 $\alpha\alpha$ ,12 $\beta\alpha$ ,12 $\alpha$ )]-5-Dimethylamino-1,5,5 $\alpha$ ,6,6 $\alpha$ ,7,12,12 $\alpha$ ,12 $\beta$ ,12 $\gamma$ -decahydro-4,7,11,12 $\beta$ ,12 $\gamma$ -penta-hydroxy-7-methyl-12-oxo-1,2-diaza-cyclopenta[de]naphthacene-3-carboxylic acid amide **2b**.** Yellowish powder, mp 280–285 °C (dec).  $t_R$  = 4.6 min.  $^1\text{H}$  NMR (500 MHz,  $\text{D}_2\text{O}$ ):  $\delta$  1.48 (q, 1H,  $J$  = 3 Hz), 1.76 (s, 3H), 2.35 (m, 2H), 2.76 (d, 1H,  $J$  = 8.8 Hz), 2.96 (s, 6H), 3.07 (d, 1H,  $J$  = 11.8 Hz), 3.75 (s, 1H), 7.04 (d, 1H,  $J$  = 8.3 Hz), 7.31 (d,  $J$  = 7.6 Hz), 7.67 (dd, 1H,  $J$  = 7.6 and 8.3 Hz).  $^{13}\text{C}$  NMR (100 MHz,  $\text{CD}_3\text{OD}$ ):  $\delta$  23.7, 29.0, 35.2, 42.4, 42.7, 53.3, 69.0, 75.7, 82.5, 86.8, 94.2, 113.8, 115.8, 117.8, 114.6, 137.5, 148.5, 157.8, 170.9, 175.3, 204.4. HRMS (ESI-TOF) calcd for  $\text{C}_{22}\text{H}_{26}\text{N}_4\text{O}_8$  459.1862 ( $\text{MH}^+$ ). Found 459.1880.

**4.3.2. [6S-(2 $\beta\alpha$ ,6 $\alpha$ ,6 $\alpha\alpha$ ,7 $\alpha\alpha$ )]-6-Dimethylamino-1,2 $\beta$ ,3,6,6 $\alpha$ ,7,7 $\alpha$ ,8-octahydro-2 $\beta$ ,5,8,12-tetrahydroxy-8-methyl-3-oxo-1,2-diaza-cyclopenta[fg]naphthacene-4-carboxylic acid amide **3b**.** Beige powder, mp 208–212 °C (dec); (lit.<sup>18</sup> mp 198–203 °C).  $t_R$  = 4.7 min.  $\lambda_{\text{max}}^{0.01\text{N HCl}}$  269, 305 nm,  $\epsilon$  25,931, 12,976. Its absorption spectrum was in good agreement with the reported one<sup>16</sup> ( $\lambda_{\text{max}}^{0.01\text{N HCl}}$  271, 306 nm,  $\epsilon$  23,600, 11,200).  $^1\text{H}$  NMR (500 MHz,  $\text{CD}_3\text{OD}$ ):  $\delta$  1.57 (s, 3H), 1.95 (m, 1H), 2.07 (m, 1H), 2.53 (s, 1H), 2.92–3.12 (m, 3H), 7.04 (d,  $J$  = 5.7 Hz, 1H), 7.12 (br s, 2H). MS (ESI),  $m/z$ : 441.2 ( $\text{MH}^+$ ).

### 4.4. Synthesis of pyrazolochlortetracycline **3c**

Chlortetracycline hydrochloride (2.0 g, 3.9 mmol) was reacted with hydrazine hydrate (2 g, 2 mL) in methanol (400 mL) at room temperature for 2 h. The resulting precipitate was filtered and treated with water (50 mL) with stirring for 1 h at room temperature to give, after filtration and thoroughly washing with water, 11,12-pyrazolochlortetracycline **3c** as a white precipitate.

**4.4.1. [6S-(2 $\beta\alpha$ ,6 $\alpha$ ,6 $\alpha\alpha$ ,7 $\alpha\alpha$ )]-9-Chloro-6-dimethylamino-1,2 $\beta$ ,3,6,6 $\alpha$ ,7,7 $\alpha$ ,8-octahydro-2 $\beta$ ,5,8,12-tetrahydroxy-8-methyl-3-oxo-1,2-diaza-cyclopenta[fg]naphthacene-4-carboxylic acid amide **3c**.** White powder, mp 291 °C (dec); (lit.<sup>16</sup> mp >300 °C).  $t_R$  = 5.7 min.  $\lambda_{\text{max}}^{0.01\text{N HCl}}$  216, 271, 316 nm,  $\epsilon$  26,525, 25,571, 10,032. Its absorption spectrum was in good agreement with the reported one<sup>18</sup> ( $\lambda_{\text{max}}^{0.01\text{N HCl}}$  216, 272, 317 nm,  $\epsilon$  26,600, 21,800, 8700).  $^1\text{H}$  NMR (500 MHz,  $\text{CD}_3\text{OD}/\text{CF}_3\text{CO}_2\text{D}$ ):  $\delta$  2.05 (q,  $J$  = 12 Hz, 1H), 2.11 (s, 3H), 2.34 (d,  $J$  = 10.1 Hz, 1H), 3.10 (s, 6H), 3.19 (m, 2H), 4.00 (s, 1H), 6.93 (d,  $J$  = 8.7 Hz, 1H), 7.73 (d,  $J$  = 8.7 Hz, 1H). MS (ESI),  $m/z$ : 475.7 ( $\text{MH}^+$ ).



#### 4.5. Crystal structure determination of compound **2b**

Pale-yellow prisms of compound **2b** were obtained upon crystallization from a tetrahydrofuran/diethyl ether system using vapor diffusion technique. A crystal with dimensions  $0.50 \times 0.15 \times 0.04$  was studied using monochromatic Mo K $\alpha$  radiation ( $\lambda = 0.71073$  Å;  $\omega$  scan mode over the  $\theta$  range of  $1.5$ – $25^\circ$ , coverage of the unique set of reflections  $>99\%$ ). No absorption correction was applied. The final unit cell parameters were calculated using the entire data set. The structure was solved by direct methods using the SHELXTL package.<sup>49</sup> Refinement (anisotropic for non-hydrogen atoms) was performed on  $F^2$  using all data with positive intensities. Hydrogen atoms were refined isotropically with thermal factors 1.2–1.5 times greater than those for the adjacent carbon atoms. The hydrogen atoms attached to carbons were fixed in the calculated positions, while the rest were unconstrained. Salient experimental details and the essential structural parameters are listed in [Supplementary data](#). Full details of the XRD analysis and complete structural information have been deposited with the Cambridge Crystallographic Data Center as CCDC 239,499. Copies of the data can be obtained, free of charge, on application to CCDC, 12 Union Road, Cambridge, CB2 1EZ, UK (fax: +44 (0)1223 336033 or e-mail: deposit@ccdc.cam.ac.uk).

#### 4.6. Assay of antibiotic activity

Two bacterial strains were used for antibiotic assay. One is the tetracycline-sensitive strain BL21(DE3), *E. coli* B F<sup>−</sup> *dem ompT hsdS* ( $r_B$ – $m_B$ ) *gal*  $\lambda$  (DE3) and the other is the tetracycline-resistant strain XL2-Blue, *recA1 endA1 gyrA96 thi-1 hsdR17 supE44 relA1 lac* [ $F'$  *proAB lacI<sup>qZ</sup>ΔM15 Tn10(Tet<sup>r</sup>) Amy Cam<sup>r</sup>*]. The bacterial strains were plated fresh from  $-80^\circ\text{C}$  glycerol stocks onto  $2 \times$  YT media agar plates (16 g/L bacto-tryptone, 10 g/L bacto-yeast extract, 5 g/L NaCl, 15 g/L bacto-agar; pH adjusted to 7.0 with NaOH) and grown overnight at  $37^\circ\text{C}$ . Single colonies of BL21(DE3) and XL2-Blue were picked and used to inoculate 7 mL flasks of LB liquid media (10 g/L bacto-tryptone, 5 g/L bacto-yeast extract, 10 g/L NaCl; pH adjusted to 7.0 with NaOH; plates contained 15 g/L bacto-agar). Cultures were grown for 6 h at 250 rpm at  $37^\circ\text{C}$  and then for 14 h at 250 rpm at  $30^\circ\text{C}$ . Bacterial concentrations were determined with a spectrophotometer and approximately 2000 CFU's of bacteria were used to incubate LB plates containing variable concentrations of compound **1a**, **b**, **2a**, or **2b** in 50% ethanol/water. Plates were incubated at  $37^\circ\text{C}$  for 20 h and then examined for bacterial growth.

#### 4.7. Zn<sup>2+</sup> binding assay

The solutions of **1a** (hydrochloride), **1b** (hydrochloride), **2a** (acetate), and **2b** (acetate) required for measuring their UV–vis absorption were obtained by mixing 0.1 mL solution of each **1a**, **b**, **2a**, or **2b** (1 mM in water) with 0.8 mL methanol and 0.1 mL of 0.05 M Tris buffer (pH 7.4) in a 1 cm quartz cuvette (1 mL volume). After the absorption curves of the four compounds were

obtained, an aliquot (10  $\mu\text{L}$ ) of ZnSO<sub>4</sub> solution (10–100 mM) was added to them to record their absorption spectra in the presence of Zn<sup>2+</sup> (0.1–1 mM). The change in volume resulted from the addition of 10  $\mu\text{L}$  ZnSO<sub>4</sub> solution to 1 mL sample was ignored. The baseline absorption spectrum was recorded with 0.1 mL water, 0.8 mL methanol, and 0.1 mL 0.05 M Tris buffer (pH 7.4), and was subtracted from the absorption spectra of the samples. The location of the maximum absorption and the change in peak heights were recorded as a function of Zn<sup>2+</sup> concentrations.

#### 4.8. Antioxidant assays

##### 4.8.1. Superoxide anion radical scavenging activity.

Superoxide radical scavenging activity was measured by employing a procedure that uses the irradiated riboflavin/EDTA/NBT system with minor modifications. The mixture consisted of 140  $\mu\text{L}$  of 0.030 mM riboflavin, 1 mM EDTA, 0.60 mM methionine and 0.030 mM NBT solution in 50 mM potassium phosphate buffer (pH 7.8) and 10  $\mu\text{L}$  of a sample solution, which includes the test compounds and the reference compounds at various concentrations in DMSO, as well as DMSO as a control. The solutions of the tested compounds had concentrations ranging from 3 to 1000  $\mu\text{g/mL}$ , whereas the concentrations of the solutions of the reference compounds varied from 0.1 to 1000  $\mu\text{g/mL}$ . The photoinduced reactions to generate superoxide anion were carried out in an aluminum foil-lined box with two 20 W fluorescent lamps. The distance between reactant and lamp was adjusted until the intensity of illumination reached 1000 lux. The reactant was illuminated at  $25^\circ\text{C}$  for 8 min. The photochemically reduced riboflavin generated superoxide anion, which reduced NBT to form the blue formazan. The un-illuminated reaction mixture was used as a blank. Reduction of NBT was measured by the absorbance change at 560 nm before and after irradiation using a microplate. Scavenging activity was calculated from the absorbance changes of control and test samples:

$$\text{Scavenging activity (\%)} = (1 - \Delta A_{\text{sample}} / \Delta A_{\text{control}}) \times 100,$$

where  $\Delta A_{\text{sample}}$  is the change of the absorbance in the wells containing the tested compounds, and  $\Delta A_{\text{control}}$  is the change of the absorbance in the wells containing the reference compounds.

The EC<sub>50</sub> value is defined as the concentration of substrate that causes 50% loss of the reduced NBT. The assays were performed in triplicate and the absorbance changes were averaged before calculation.

##### 4.8.2. DPPH radical scavenging activity.

DPPH radical scavenging activity was determined using the method of Brand-Williams et al.<sup>35</sup> with minor modifications. The solution of the sample (10  $\mu\text{L}$ ) in ethanol was added to 90  $\mu\text{L}$  of a 0.15 mM DPPH radical in ethanol in a 96-well plate. The sample solution refers to the tested compounds and the reference antioxidants at various concentrations, as well as ethanol as a control. The solutions of the tested compounds had concentrations

ranging from 3 µg/mL to 1000 µg/mL, whereas the concentrations of the solutions of the reference compounds varied from 0.1 µg/mL to 1000 µg/mL. The reaction leading to the scavenging of DPPH radical was complete within 10 min at 25 °C. The absorbance of the mixture was then measured at 517 nm using a microplate reader. The reduction of DPPH radical was expressed as percentage:

$$\text{Scavenged DPPH (\%)} = (1 - A_{\text{test}}/A_{\text{control}}) \times 100,$$

where  $A_{\text{test}}$  is the absorbance of a sample at a given concentration after 10 min reaction time and  $A_{\text{control}}$  is the absorbance recorded for 10 µL ethanol. The  $EC_{50}$  value is defined as the concentration of sample that causes 50% loss of the DPPH radical.

**4.8.3. ABTS cation radical scavenging activity.** The ABTS cation radical was produced by the reaction between 7.0 mM ABTS/water and 2.45 mM potassium persulfate for 12 h in the dark at room temperature. The  $ABTS^{+}$  solution was diluted with PBS until  $A_{734} = 0.7$ . The reaction was initiated by adding 190 µL of  $ABTS^{+}$  solution to 10 µL sample solution at 25 °C. The percentage of reduction of  $A_{734}$  was recorded and was plotted as a function of the sample's concentration.

### Acknowledgments

We acknowledge our colleagues Drs. Takahiro Kubo and Angela Angusti for their helpful discussions. We thank Dr. Cristina Draghici for her technical assistance with the mass spectrometry analysis. We are grateful to National Sciences and Engineering Research Council of Canada for the financial support of this work.

### Supplementary data

The molecular structure and ORTEP drawing of compound **2b**, summary of the single-crystal XRD analysis, and hydrogen-bond geometry are available via the Internet. Supplementary data associated with this article can be found in the online version at [doi:10.1016/j.bmc.2005.04.032](https://doi.org/10.1016/j.bmc.2005.04.032).

### References and notes

- Palinski, W.; Rosenfeld, M. E.; Ylä-Herttuala, S.; Gurtner, G. C.; Socher, S. S.; Butler, S. W.; Parthasarathy, S.; Carew, T. E.; Steinberg, D.; Witztum, J. L. *Proc. Natl. Acad. Sci. U.S.A.* **1989**, *86*, 1372.
- Cheeseman, K. H.; Forni, L. G. *Biochem. Pharmacol.* **1988**, *37*, 4225.
- Weitzman, S. A.; Weitberg, A. B.; Clark, E. P.; Stossel, T. P. *Science* **1985**, *227*, 1231.
- Fantone, J. C.; Ward, P. A. *Hum. Pathol.* **1985**, *16*, 973.
- Cengiz, M.; Seven, M.; Suyugul, N. *Genet. Couns.* **2002**, *13*, 339.
- Sharma, A.; Bansal, S.; Nagpal, R. K. *Indian J. Pediatr.* **2003**, *70*, 715.
- Tretter, L.; Sipos, I.; Adam-Vizi, V. *Neurochem. Res.* **2004**, *29*, 569.
- Zhu, X.; Raina, A. K.; Perry, G.; Smith, M. A. *Lancet Neurol.* **2004**, *3*, 219.
- Canevari, L.; Abramov, A. Y.; Duchon, M. R. *Neurochem. Res.* **2004**, *29*, 637.
- Wiernsperger, N. F. *Biofactors* **2003**, *19*, 11.
- Mossine, V. V.; Linetsky, M.; Glinsky, G. V.; Ortwerth, B. J.; Feather, M. S. *Chem. Res. Toxicol.* **1999**, *12*, 230.
- Guo, Q.; Packer, L. *Free Radical. Biol. Med.* **2000**, *29*, 368.
- Chan, A. C.; Chow, C. K.; Chiu, D. *Proc. Soc. Exp. Biol. Med.* **1999**, *222*, 274.
- Pioletti, M.; Schlunzen, F.; Harms, J.; Zarivach, R.; Gluhmann, M.; Avila, H.; Bashan, A.; Bartels, H.; Auerbach, T.; Jacobi, C.; Hartsch, T.; Yonath, A.; Franceschi, F. *EMBO J.* **2001**, *20*, 1829.
- Ryan, M. E.; Usman, A.; Ramamurthy, N. S.; Golub, L. M.; Greenwald, R. A. *Curr. Med. Chem.* **2001**, *8*, 305.
- Pozzi, A.; LeVine, W. F.; Gardner, H. A. *Oncogene* **2002**, *21*, 272.
- Elguero, J. Pyrazoles. In *Comprehensive Heterocyclic Chemistry II: a Review of the Literature 1982–1995: the Structure, Reactions, Synthesis, and Uses of Heterocyclic Compounds*; Katritzky, A. R., Rees, C. W., Scriven, E. F. V., Eds.; Pergamon: New York, 1996; Vol. 3, pp 1–75.
- Valcavi, U.; Campanella, G.; Pacini, N. *Gazz. Chim. Ital.* **1963**, *93*, 916.
- Katritzky, A. R.; Osterkamp, D. L.; Yousaf, T. I. *Tetrahedron* **1987**, *43*, 5171.
- Singh, S. P.; Kumar, D.; Batra, H.; Naithani, R.; Rozas, I.; Elguero, J. *Can. J. Chem.* **2000**, *78*, 1109.
- Stezowski, J. J. *J. Am. Chem. Soc.* **1976**, *98*, 6012.
- Gulbis, J.; Everett, G. W., Jr. *Tetrahedron* **1976**, *32*, 913.
- Prew, R.; Stezowski, J. J. *J. Am. Chem. Soc.* **1977**, *99*, 1117.
- Spahn, C. M. T.; Prescott, C. D. *J. Mol. Med.* **1996**, *74*, 423.
- Brodersen, D. E.; Clemons, W. M., Jr.; Carter, A. P.; Morgan-Warren, R. J.; Wimberly, B. T.; Ramakrishnan, V. *Cell* **2000**, *103*, 1143.
- White, J. P.; Cantor, C. R. *J. Mol. Biol.* **1971**, *58*, 397.
- Golub, L. M.; Ramamurthy, N. S.; McNamara, T. F.; Greenwald, R. A.; Rifkin, B. R. *Crit. Rev. Oral Biol. Med.* **1991**, *2*, 297.
- Golub, L. M.; Lee, H. M.; Ryan, M. E.; Giannobile, W. V.; Payne, J.; Sorsa, T. *Adv. Dent. Res.* **1998**, *12*, 12.
- Greenwald, R. A.; Golub, L. M.; Ramamurthy, N. S.; Chowdhury, M.; Moak, S. A.; Sorsa, T. *Bone* **1998**, *22*, 33.
- Sorsa, T.; Ramamurthy, N. S.; Vernillo, A. T.; Zhang, X.; Kontinen, Y. T.; Rifkin, B. R.; Golub, L. M. *J. Rheumatol.* **1998**, *25*, 975.
- Lukkonen, A.; Sorsa, T.; Salo, T.; Tervahartiala, T.; Koivunen, E.; Golub, L.; Simon, S.; Stenman, U. H. *Int. J. Cancer* **2000**, *86*, 577.
- Yu, L. P., Jr.; Smith, G. N., Jr.; Hasty, K. A.; Brandt, K. D. *J. Rheumatol.* **1991**, *18*, 1450.
- Ryan, M. E.; Ramamurthy, S.; Golub, L. M. *Curr. Opin. Periodontol.* **1996**, *3*, 85.
- Lovejoy, B.; Cleasby, A.; Hassell, A. M.; Longley, K.; Luther, M. A.; Weigl, D.; McGeehan, G.; McElroy, A. B.; Drewry, D.; Lambert, M. H.; Jordan, S. R. *Science* **1994**, *263*, 375.
- Swann, J. C.; Reynolds, J. J.; Galloway, W. A. *Biochem. J.* **1981**, *195*, 41.
- Katakwar, T. K.; Kacchawaha, M. S. *Hindustan Antibiot. Bull.* **1984**, *26*, 9.
- Tongaree, S.; Flanagan, D. R.; Poust, R. I. *Pharm. Dev. Technol.* **1999**, *4*, 581.

38. Brion, M.; Lambs, L.; Berthon, G. *Agents Actions* **1985**, *17*, 229.
39. Novák-Pékli, M.; El-Hadi Mesbah, M.; Pethő, G. *J. Pharm. Biomed. Anal.* **1996**, *14*, 1025.
40. Caswell, A. H.; Hutchison, J. D. *Biochem. Biophys. Res. Commun.* **1971**, *43*, 625.
41. *Free Radical and Antioxidant Protocols*; Armstrong, D., Ed.; Humana: Totowa, NJ, 1988.
42. Brand-Williams, W.; Cuvelier, M. E.; Berset, C. *Lebensm.-Wiss. u.-Technol.* **1995**, *28*, 25.
43. Re, R.; Pellegrini, N.; Proteggente, A.; Pannala, A.; Yang, M.; Rice-Evans, C. *Free Radical. Biol. Med.* **1999**, *26*, 1231.
44. Beauchamp, C.; Fridovich, I. *Anal. Biochem.* **1971**, *44*, 276.
45. Sum, P. E.; Sum, F. W.; Projan, S. J. *Curr. Pharm. Des.* **1998**, *4*, 119.
46. Matter, H.; Schudok, M. *Curr. Opin. Drug Disc. Dev.* **2004**, *7*, 513.
47. Galis, Z. S.; Khatri, J. J. *Circ. Res.* **2002**, *90*, 251.
48. Bernier, C.; Dreno, B. *Ann. Dermatol. Venereol.* **2001**, *128*, 627.
49. Sheldrick, G. M. *SHELXTL PC, Ver. 4 1. An integrated system for solving, refining and displaying crystal structure from diffraction data*. Siemens Analytical X-ray Instruments, Inc., Madison, WI, 1990.